Electronic Supplementary Material (ESI) for Physical Chemistry Chemical Physics.

Electronic Supplementary Information

Fluorescence enhancement in Visible Light: Dielectric or Noble Metal?

Song Sun, Lin Wu, Ping Bai and Ching Eng Png*

Electronics and Photonics Department, Institute of High Performance Computing, Agency for Science, Technology and Research, 138632, Singapore

*Corresponding author, Email: baiping@ihpc.a-star.edu.sg

1. Mode compositions of 125 nm Si, 90 nm Si and 130 nm Ag NPs in the air medium and modes excited by an electric dipole

Fig. S1 top row shows the detail mode compositions of (a) 125 nm Si, (b) 90 nm Si, and (c) 130 nm Ag NPs in the air medium, which are calculated based on the Mie coefficients described in the Methods section of the main text. The separate contribution of the electric dipole (ED), magnetic dipole (MD), electric quadrupole (EQ) and magnetic quadrupole (MQ) are illustrated. Clearly, the Ag NP has predominant ED and negligible magnetic response due to the pure electric nature of the plasmonic resonance. On the other hand, the Si NP can possess both the ED and MD at the same time. Note that the ED of 125 nm Si, the MD of 90 nm Si as well as the plasmonic resonance of 130 nm Ag are all located at 445 nm (the excitation wavelength used in Fig. 1 of the main text) to ensure a fair comparison.

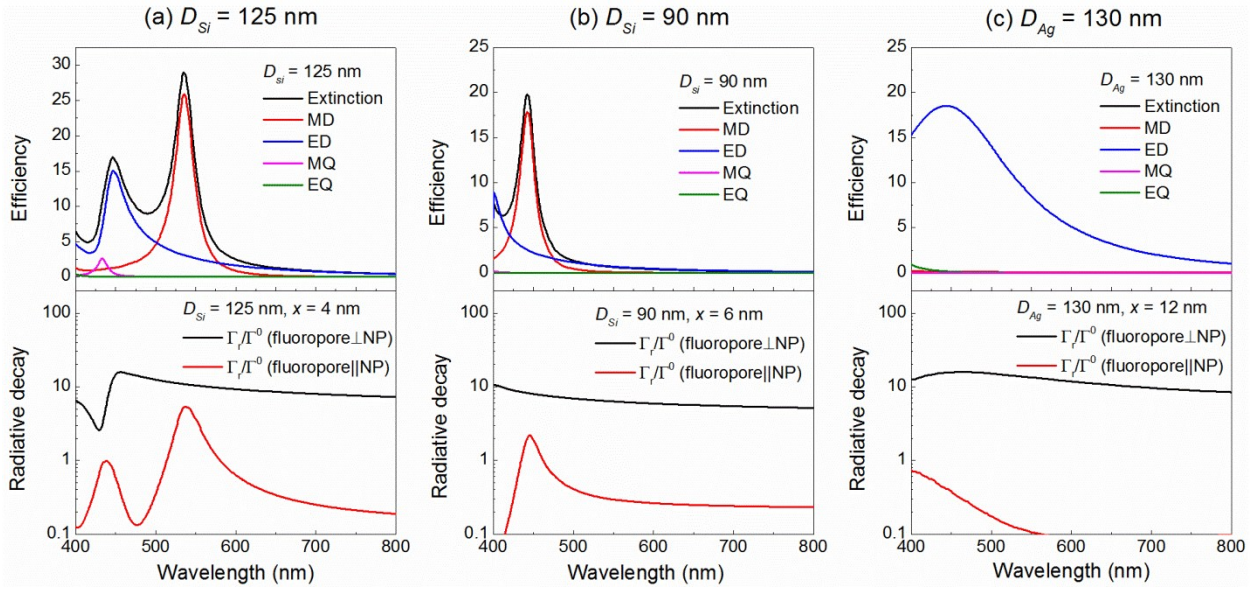

Fig. S1 The resonance mode composition (top row) and the excitation of these modes by an electric dipole (bottom row) for: (a) a 125 nm Si NP, (b) a 90 nm Si NP and (c) a 130 nm Ag NP. The separate contribution of electric dipole (ED), magnetic dipole (MD), electric quadrupole (EQ) and magnetic quadrupole (MQ) are illustrated. A

perpendicular dipole can strongly excite the ED of the Si NP and the plasmonic resonance of the Ag NP, whereas a parallel dipole can only weakly excite the MD of the Si NP.

Under electric dipole radiation, the excitations of these modes are illustrated in their corresponding radiative decay rates Γ_r/Γ^0 as shown in Fig. S1 bottom row. Clearly, a dipole oriented perpendicular to the NP (fluorophore⊥NP) can strongly excite the ED of the Si NP as well as the SPR of the Ag NP, resulting in a high Γ_r/Γ^0. The maximum Γ_r/Γ^0 is achieved when the fluorescence emission wavelength is consistent with the Si ED or the SPR of plasmonic NP. Γ_r/Γ^0 gradually decreases as the fluorescence emission wavelength moves away from the resonance mode (ED, MD and SPR) of NP to longer wavelength.

On the other hand, a dipole parallel to the NP (fluorophore||NP) can only weakly excite the MD of the Si NP, and have little effect on the SPR of Ag NP or the ED of Si NP. As a result, Γ_r/Γ^0 is much smaller as compared to that of fluorophore⊥NP and extended over a much narrower spectrum region. Even for Si MD which is excited for fluorophore||NP, Γ_r/Γ^0 is still much weaker than that for fluorophore⊥NP. Note that our conclusions are consistent with the results published previously by Schmidt et al.[1]

2. The permittivity and conductivity of some commonly used dielectric materials in the visible light region

Fig. S2 shows (a) the permittivity and (b) conductivity profile of some commonly used dielectric materials in the visible light spectrum, whereby the material properties are taken from online database.[2] Among these materials, Si possesses relatively large permittivity as well as low

conductivity in the visible light region. Therefore, we believe Si is the best choice for fluorescence enhancement. The conductivity σ can be obtained as $\sigma = \omega\varepsilon_0\varepsilon''_{NP}$,[3] where ω is the optical frequency, ε_0 is the free space permittivity and ε''_{NP} is the imaginary part of the complex permittivity of the NP's material.

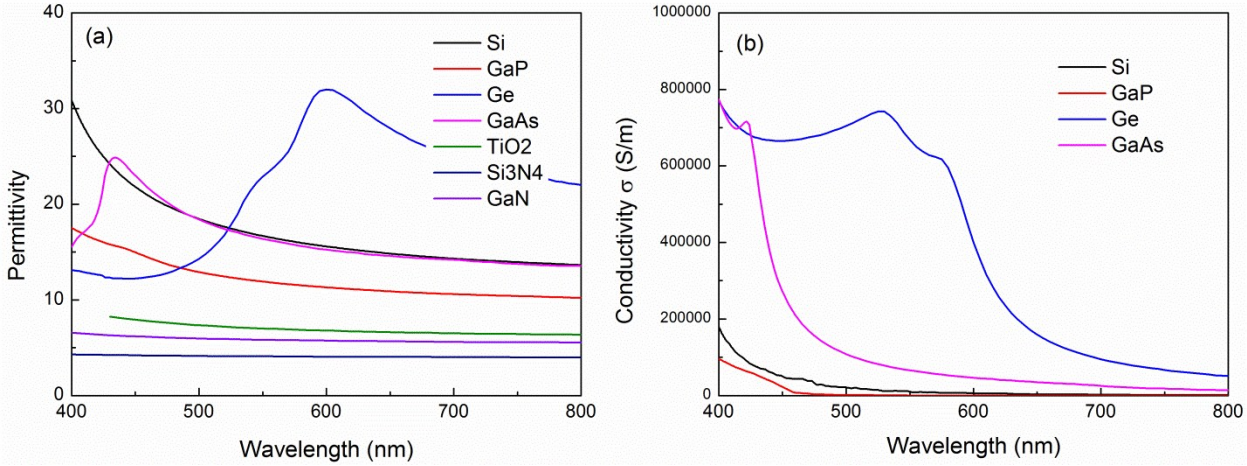

Fig. S2. The (a) permittivity and (b) conductivity profile of some commonly used dielectrics in the visible light region.

3. The decay rates and quantum yield for fluorophore oriented parallel to the NP at λ_{em} = 445 nm

Fig. S3 shows (a) the decay rates and (b) the quantum yield for fluorophore oriented parallel ('||') to the NP at λ_{em} = 445 nm. Since a parallel electric dipole can only weakly excite the MD of Si NP and has negligible effect on the SPR of Ag NP or the ED of Si NP (see Fig. S1 bottom row),[3] the magnitudes of the decay rates (both Γ_r/Γ^0 and Γ_{nr}/Γ^0) and quantum yield q/q^0 are much smaller as compared to those for fluorophore⊥NP (see Fig. 2 in the main text). In particular, the radiative decay rates Γ_r/Γ^0 drop approximately one order of magnitude. This

clearly indicates that the maximum fluorescence enhancement and the highest radiative decay rate can only be achieved when the fluorophore aligns perpendicular to the NP.

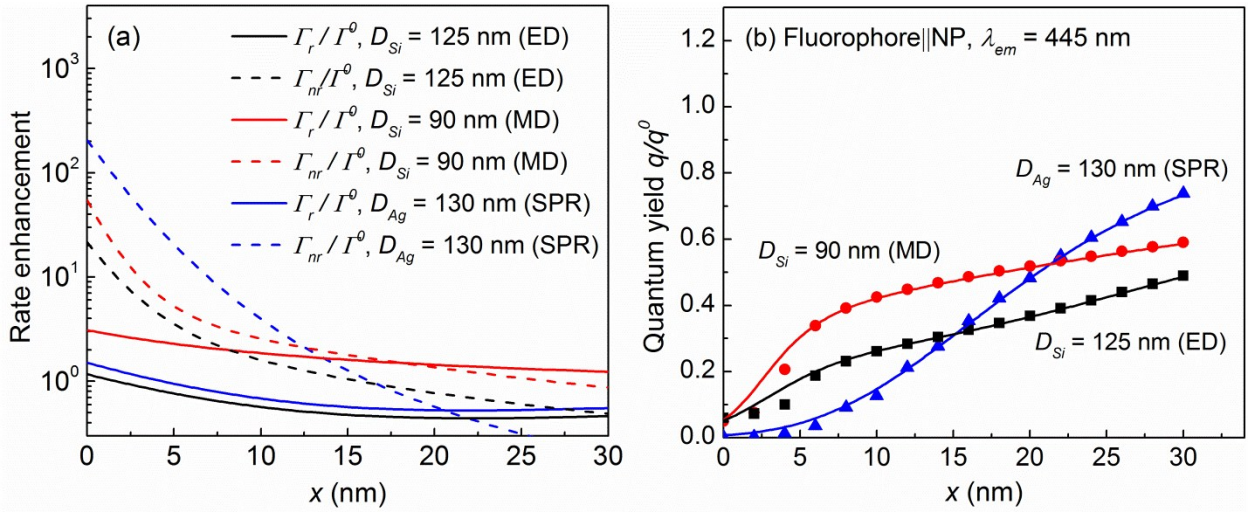

Fig. S3. (a) The decay rates and (b) the quantum yield for fluorophore oriented parallel ('||') to the NP at fluorescence emission wavelength λ_{em} = 445 nm. The respective quantum yield and decay rates of the three NPs are much smaller than those of fluorophore⊥NP because a parallel electric dipole can only weakly excite the MD of a dielectric NP.

4. Mode compositions of 175 nm Si, 130 nm Si and 160 nm Au NPs in air medium

Fig. S4 shows the detail mode compositions of (a) 175 nm Si, (b) 130 nm Si, and (c) 160 nm Au NPs in air medium. The separate contribution of the electric dipole (ED), magnetic dipole (MD), electric quadrupole (EQ) and magnetic quadrupole (MQ) are illustrated. The ED of 175 nm Si, MD of 130 nm Si as well as the plasmonic resonance of 160 nm Au are all located at 550 nm (the excitation wavelength used in Fig. 4 of the main text) to ensure a fair comparison.

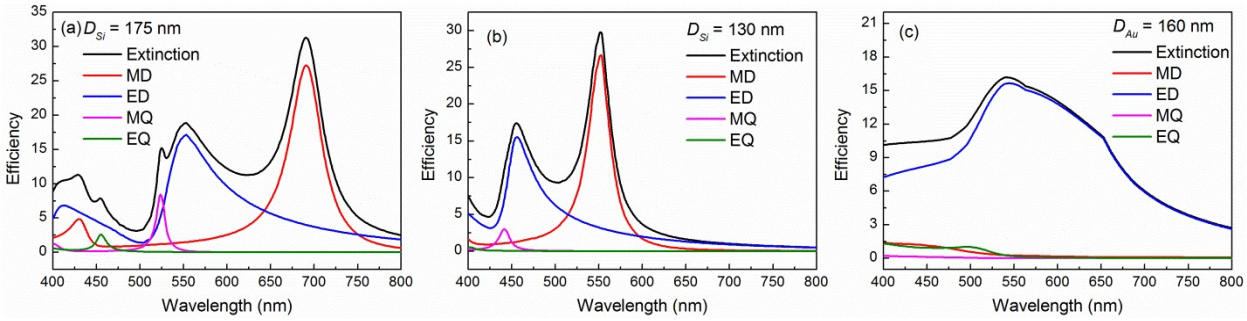

Fig. S4. The mode compositions of (a) 175 nm Si, (b) 130 nm Si and (c) 160 nm Au NPs. The contributions of electric dipole, magnetic dipole, electric quadrupole and magnetic quadrupole are denoted as ED, MD, EQ and MQ respectively.

5. Enhance the quantum yield at low conductivity region of plasmonic NP

Fig. S5 extends the same idea in Fig. 3 in the main text to the plasmonic NP, whereby the quantum yield can be enhanced by reducing the loss at low conductivity region. Fig. S5 (a) shows the conductivity profiles of Au and Ag in the visible light region. The conductivity of Au decreases fast as wavelength increases, and reaches a low level for wavelength beyond 650 nm. Therefore, it is expected that the loss or nonradiative decay rate of the Au NP is greatly suppressed at long fluorophore emission wavelength λ_{em}, and its quantum yield can be significantly improved as shown in Fig. S5 (b). On the other hand, the conductivity of Ag is approximately constant over the visible light region. As a result, the quantum yield of the Ag NP does not change much at different wavelengths as shown in Fig. S5 (c). Note that the sizes of NPs are designed so that the plasmonic resonances of the NPs are the same as the fluorophore emission wavelength λ_{em}.

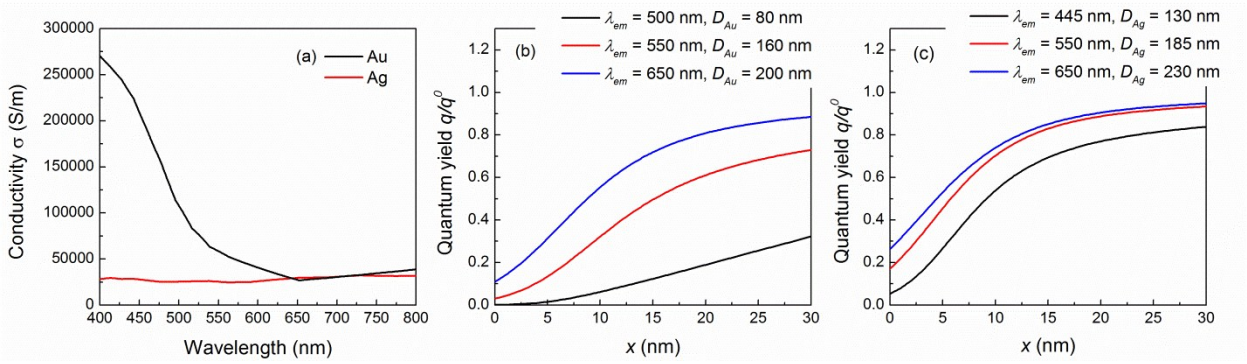

Fig. S5. (a) The conductivity profiles of Au and Ag in the visible light region. (b) The quantum yields of Au NPs at various fluorescence emission wavelength λ_{em}. The quantum yield of the Au NP is significantly improved at longer λ_{em} due to the giant decrement on the conductivity. (c) The quantum yields of Ag NPs at various fluorescence emission wavelength λ_{em}. The quantum yield of the Ag NP does not change much since its conductivity is approximately constant over the visible light region.

6. Mode compositions of the 165 nm Si, 130 nm Si and 125 nm Ag NPs in the water medium

Fig. S6 shows the detail mode compositions of (a) 165 nm Si, (b) 130 nm Si, and (c) 125 nm Ag NPs in water medium. The separate contribution of electric dipole (ED), magnetic dipole (MD), electric quadrupole (EQ) and magnetic quadrupole (MQ) are illustrated. The ED of 165 nm Si, MD of 130 nm Si as well as the plasmonic resonance of 125 nm Ag are all located at 550 nm (the excitation wavelength used in Fig. 6 of the main text) to ensure a fair comparison.

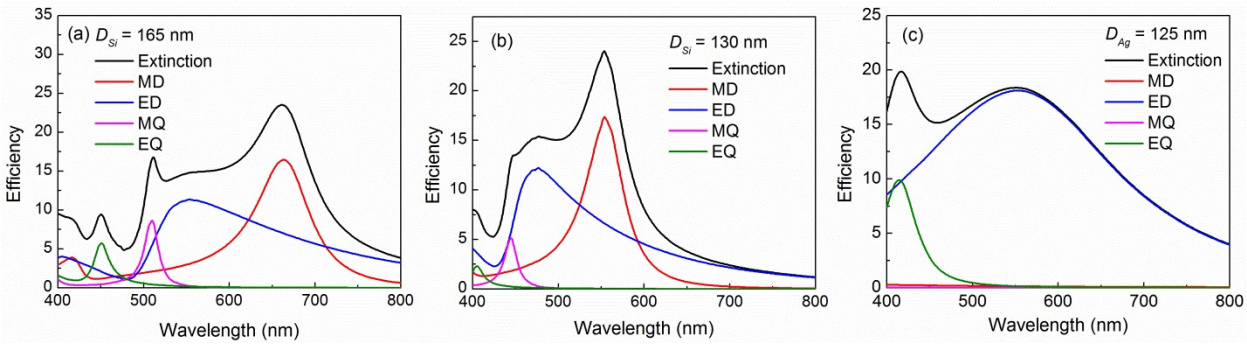

Fig. S6. The mode compositions of (a) 165 nm Si, (b) 130 nm Si and (c) 125 nm Ag NPs. The contributions of electric dipole, magnetic dipole, electric quadrupole and magnetic quadrupole are denoted as ED, MD, EQ and MQ respectively.

7. Change in the extinction spectrum of the Si NP with respect to the permittivity of medium

Fig. S7 shows the change in the extinction spectrum of a 165 nm Si NP as the permittivity of the medium gradually increases from (a) ε_m = 1 (air) to (b) ε_m = 1.77 (water) and (c) ε_m = 2.25 (oil). Apparently, the extinction efficiency of the Si ED decreases tremendously as ε_m increases, which completely smears out in the oil medium. The Si MD, although still remains well-resolved, also suffers a significant decrement in the extinction efficiency. This explains why the NP-enhanced excitation rate of the Si NP becomes smaller when immerging in a high index medium, in particular for the Si ED. Note that our calculations are consistent with the results published previously by Sáenz et al.[4]

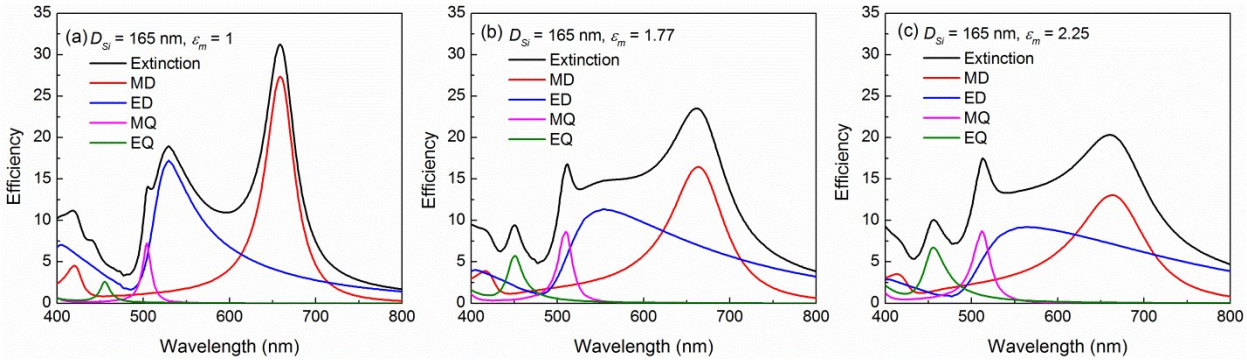

Fig. S7. The change in the extinction spectrum of a 165 nm Si NP as the permittivity of the medium gradually increases from (a) ε_m = 1 (air) to (b) ε_m = 1.77 (water) and (c) ε_m = 2.25 (oil).

8. NP-enhanced fluorescence at 650 nm in water medium

Below we compare the NP-enhanced fluorescence at $\lambda_{ext} = \lambda_{em} = 650$ nm in water medium, which corresponds to the ED of a 205 nm Si, MD of a 160 nm Si, and SPR of a 130 nm Au NP as shown in Fig. S8 (a). The NP-enhanced excitation rate $\gamma_{ext}/\gamma^0_{ext}$ is shown in Fig. S8 (b), which demonstrates that $\gamma_{ext}/\gamma^0_{ext}$ of the Si NP decrease significantly (especially Si ED) in water medium and are much smaller than that of the Au NP. Although the quantum yields q/q^0 of the Si NP are higher than that of the Au NP due to the low conductivity of Si at 650 nm (see Fig. S8 (c)), it is not enough to compensate the reduction on $\gamma_{ext}/\gamma^0_{ext}$. Therefore, the fluorescence enhancement η_{em}/η^0_{em} and far field emission pattern of the Si NP in water medium are weaker than those of the Au NP as shown in Fig. S8 (d) and (e) respectively.

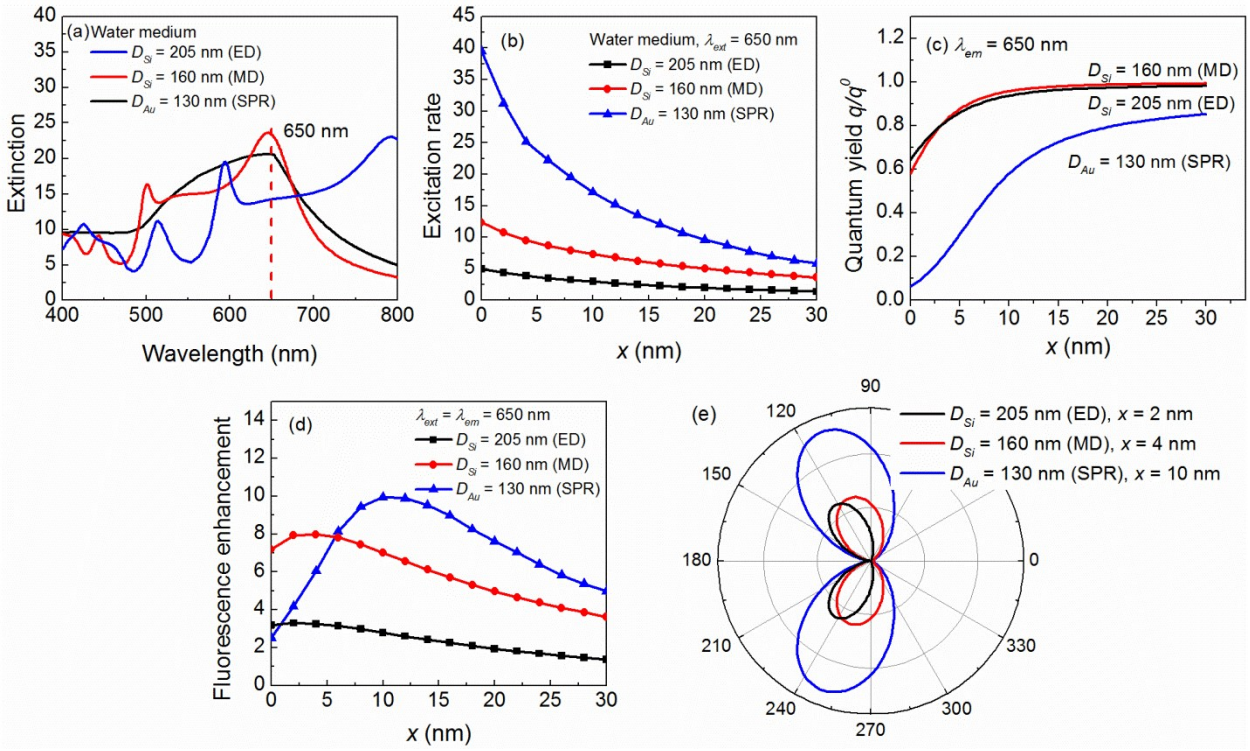

Fig. S8. (a) The extinction spectrum of NPs in water medium. The ED of 205 nm Si, the MD of 160 nm Si and SPR of 130 nm Au NP are controlled at λ_{ext} = 650 nm to ensure a fair comparison. (b) The NP-enhanced excitation rate $\gamma_{ext}/\gamma^0_{ext}$ of the Si NP decrease significantly (especially Si ED) in water medium and are much smaller than that of the Au NP. (c) The quantum yields q/q^0 of the Si NP are higher than that of the Au NP due to the low conductivity of Si at 650 nm, but it is not enough to compensate the reduction on $\gamma_{ext}/\gamma^0_{ext}$. (d) The fluorescence enhancement η_{em}/η^0_{em} and (e) far field emission pattern of the Si NP in water medium are weaker than those of the Au NP.

9. Fluorophores with large stokes shifts in water medium

Fig. S9 below shows the fluorescence enhancement for fluorophores with large stokes shifts in water medium. Here we assume λ_{ext} = 550 nm which corresponds to the ED of a 165 nm Si and the SPR of a 125 nm Ag in water medium (see Figure 4a in the main text), and vary λ_{em} = 550 nm and 650 nm. Fig. S9 (a) shows the corresponding quantum yields q/q^0 for the Si (solid line) and Ag NP (dashed line) respectively. The q/q^0 of the Si NP is larger than that of the Ag NP since the conductivity of Si is generally much smaller than that of Ag. Multiplying the NP-enhanced fluorescence excitation rate $\gamma_{ext}/\gamma^0_{ext}$ at λ_{ext} = 550 nm (Fig. 4b in the main text), the resultant fluorescence enhancements η_{em}/η^0_{em} are shown in Fig. S9 (b) for the Si NP and the Ag NP. Clearly in the water medium, the Si NP cannot generate higher η_{em}/η^0_{em} than the Ag NP due to the giant decrement on the NP-enhanced excitation rate regardless of the stoke shifts.

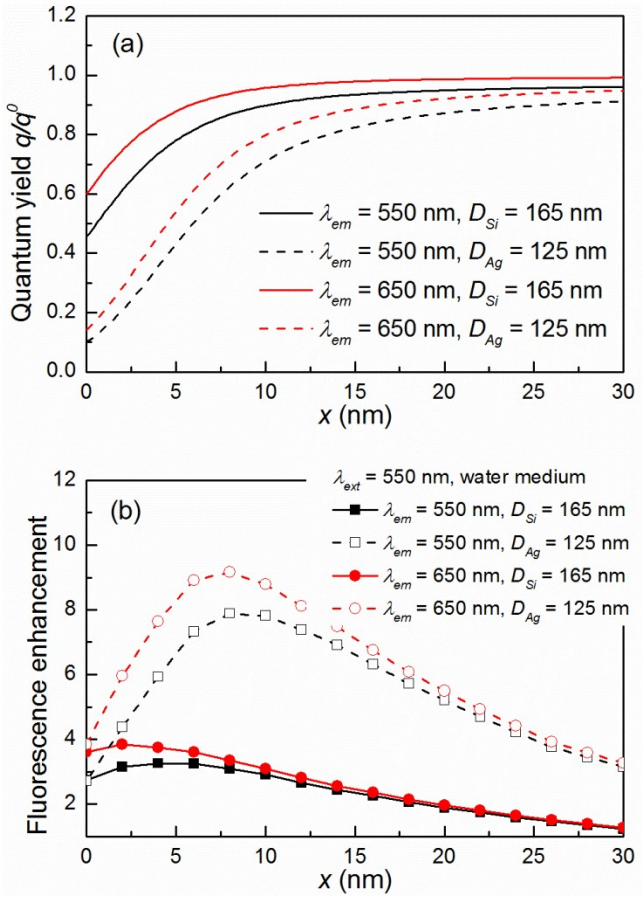

Fig. S9. (a) The quantum yield q/q^0 for a 165 nm Si (ED = 550 nm) and a 125 nm Ag (SPR = 550 nm) in water medium at fixed fluorescence excitation wavelength λ_{ext} = 550 nm and various fluorescence emission wavelengths λ_{em} = 550 nm and 650 nm. (b) The respective fluorescence enhancements η_{em}/η^0_{em} for the Si NP (solid line with closed symbol) and the Ag NP (dashed line with open symbol). Regardless of the fluorescence stokes shift, the Si NP cannot outperform the Ag NP in water medium due to the giant decrement on the NP-enhanced excitation rate.

10. Far field intensity for plasmonic NP with different fluorescence emission wavelength

Fig. S10 below shows the far field intensity for a 130 nm Ag NP (SPR aligns at λ_{ext} = 445 nm) with different fluorescence stokes shifts (λ_{em} = 445 nm, 550 nm and 650 nm). Similar to the Si ED (Fig. 6d in the main text), if fluorophores with large stokes shifts are used, a longer

emission wavelength λ_{em} leads to a smaller far field intensity because it is off-resonance of the SPR of the Ag NP.

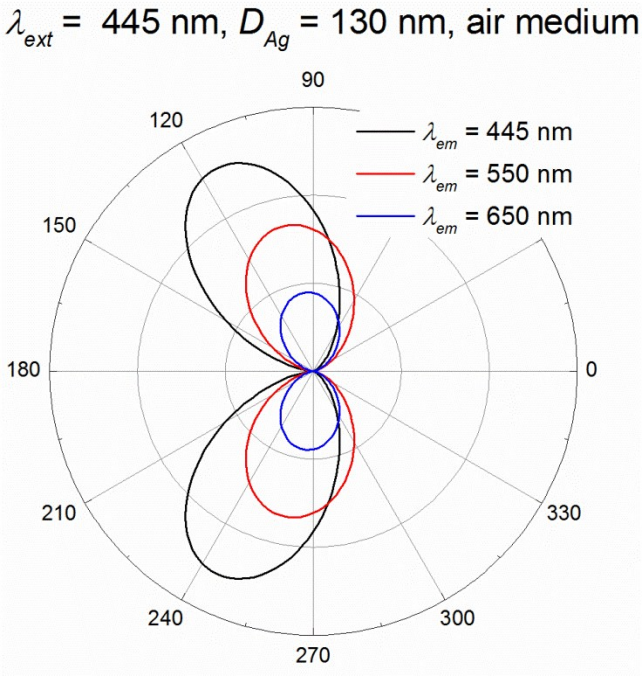

Fig. S10. The far field intensities for fluorophore wavelengths at λ_{ext} = 445 nm and λ_{em} = 445 nm, 550 nm and 650 nm in air medium for a 130 nm Ag NP (SPR aligns at λ_{ext} = 445 nm).

11. Minimum requirement on the dielectric permittivity to outperform plasmonic metal

The general guideline on the minimum permittivity requirement reported in Fig. 7 in the main text also holds at other wavelengths. Fig. S11 below shows that (a) in the air medium, a minimum ε_{NP} of 9 is identified to guarantee a higher η_{em}/η^0_{em} than that of the Au NP at $\lambda_{ext} = \lambda_{em}$ = 550 nm, and (b) in the water medium, it must be at least of 16 to outperform the Au NP at $\lambda_{ext} = \lambda_{em}$ = 650 nm.

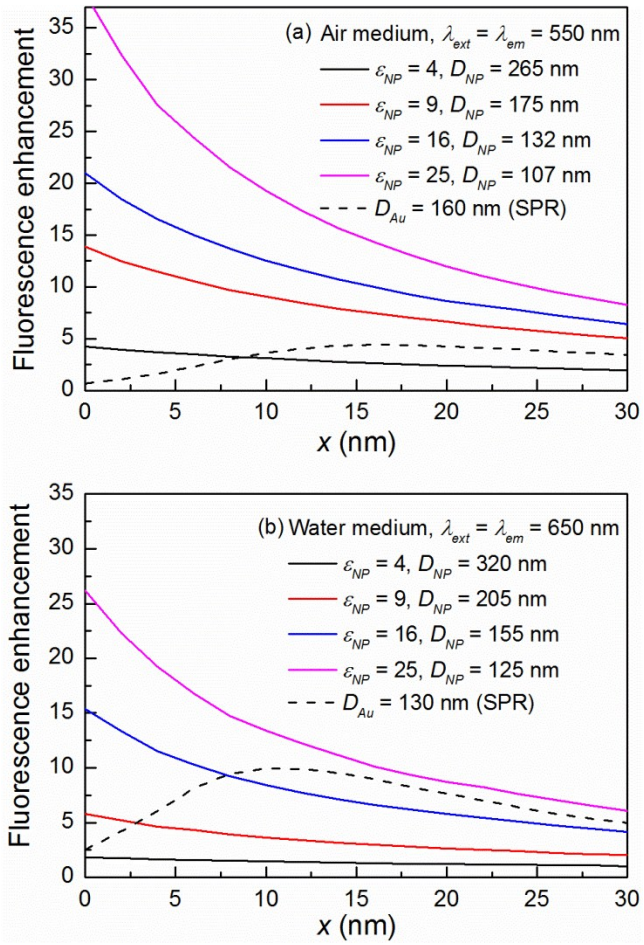

Fig. S11. The general guideline on the minimum requirement on the permitivities ε_{NP} of an absolutely lossless dielectric NP to outperform plasmonic NP in the (a) air medium for $\lambda_{ext} = \lambda_{em}$ = 445 nm and (b) water medium for $\lambda_{ext} = \lambda_{em}$ = 650 nm.

References

1. Schmidt, M. K.; Esteban, R.; Sáenz, J. J.; Suárez-Lacalle, I.; Mackowski, S.; Aizpurua, J. *Opt. Express* **2012**, *20*, 13636-13650.
2. http://refractiveindex.info/
3. Ruppin, R; *J. Chem. Physics*, **1982**, *76*, 1681-1684.
4. García-Etxarri, A.; Gómez-Medina, R.; Froufe-Pérez, L. S.; López, C.; Chantada, L.; Aizpurua, J.; Nieto-Vesperinas, M.; Sáenz, J. J. *Opt. Express* **2011**, *19*, 4815-4826.